Reappraising myocardial fibrosis in severe aortic stenosis: an invasive and non-invasive study in 133 patients

Thomas A. Treibel[1,2]†, Begoña López[3,4]†, Arantxa González[3,4]†, Katia Menacho[1], Rebecca S. Schofield[1], Susana Ravassa[3,4], Marianna Fontana[2], Steven K. White[2], Carmelo DiSalvo[1], Neil Roberts[1], Michael T. Ashworth[2,5], Javier Díez[3,4,6], and James C. Moon[1,2]*

[1]Cardiac Imaging, Barts Heart Centre, St. Bartholomew's Hospital, 2nd Floor, King George V Block, Barts Heart Centre, St. Bartholomew's Hospital, London EC1A 7BE, UK; [2]Institute for Cardiovascular Sciences, University College London, Gower Street, London WC1E 6BT, UK; [3]Program of Cardiovascular Diseases, Center for Applied Medical Research, University of Navarra, Avda/ Pío XII 55, 31008, Pamplona, Spain; [4]CIBERCV, National Institute of Health Carlos III, C/ Monforte de Lemos 3-5, 28029, Madrid, Spain; [5]Department of Histopathology, Great Ormond Street Hospital for Children National Health Service Trust, Great Ormond Street, London WC1N 3JH, UK; and [6]Department of Cardiology and Cardiac Surgery, University of Navarra Clinic, Avda/ Pío XII 36, 31008, Pamplona, Spain

Aims	To investigate myocardial fibrosis (MF) in a large series of severe aortic stenosis (AS) patients using invasive biopsy and non-invasive imaging.
Methods and results	One hundred thirty-three patients with severe, symptomatic AS accepted for surgical aortic valve replacement underwent cardiovascular magnetic resonance (CMR) with late gadolinium enhancement (LGE) and extracellular volume fraction (ECV) quantification. Intra-operative left ventricular (LV) biopsies were performed by needle or scalpel, yielding tissue with ($n = 53$) and without endocardium ($n = 80$), and compared with 10 controls. Myocardial fibrosis occurred in three patterns: (i) thickened endocardium with a fibrotic layer; (ii) microscopic scars, with a subendomyocardial predominance; and (iii) diffuse interstitial fibrosis. Collagen volume fraction (CVF) was elevated ($P < 0.001$) compared with controls, and higher ($P < 0.001$) in endocardium-containing samples with a decreasing CVF gradient from the subendocardium ($P = 0.001$). Late gadolinium enhancement correlated with CVF ($P < 0.001$) but not ECV. Both LGE and ECV correlated independently ($P < 0.001$) with N-terminal pro-brain natriuretic peptide and high-sensitivity-troponin T. High ECV was also associated with worse LV remodelling, left ventricular ejection fraction and functional capacity. Combining high ECV and LGE better identified patients with more adverse LV remodelling, blood biomarkers and histological parameters, and worse functional capacity than each parameter alone.
Conclusion	Myocardial fibrosis in severe AS is complex, but three main patterns exist: endocardial fibrosis, microscars (mainly in the subendomyocardium), and diffuse interstitial fibrosis. Neither histological CVF nor the CMR parameters ECV and LGE capture fibrosis in its totality. A combined, multi-parametric approach with ECV and LGE allows best stratification of AS patients according to the response of the myocardial collagen matrix.
Keywords	Myocardial fibrosis • Aortic stenosis • Cardiovascular magnetic resonance • Late gadolinium enhancement • Extracellular volume fraction

---

Introduction

In aortic stenosis (AS), patient symptoms and outcome are determined by the severity of the valve stenosis, but also by the myocardial response to the generated afterload—a process that appears crucial, but is incompletely understood.[1] Our scientific exploration of this uses two main approaches. Clinically, the myocardium is measured by assessing structure and function using imaging [echocardiography, cardiovascular magnetic resonance (CMR)].[2] Pathophysiologically, the myocardium is assessed histologically on tissue samples. It is believed that a complex interplay of cellular changes (including hypertrophy and cell death by apoptosis or autophagy), microvascular ischaemia, and alterations of the extracellular matrix occurs with final common pathways leading to myocardial fibrosis (MF). Most of the evidence for this has been from a few small biopsy or autopsy studies. Whereas autopsy descriptions of MF can provide a global view, in *in vivo* studies, sampling is limited by biopsy size, and fibrosis is typically described only by the quantity of collagen deposition [collagen volume fraction (CVF)]. However, histological analysis of heart tissue also allows differentiation of fibrosis subtypes based on location and morphological characteristics of collagen deposits (focal microscopic scars, diffuse interstitial and perivascular strands; see Supplementary material online, *Figure S1*), with the functional impact of MF not only depending on the amount of collagen tissue but also on the characteristics of collagen deposits.[3] Although new insights are being generated by imaging tissue characterization [the late gadolinium enhancement (LGE) technique permits quantification of focal interstitial expansion,[4–8] and diffuse interstitial expansion can be measured by extracellular volume fraction (ECV)[9–12]], the histological basis of LGE and ECV in AS and their association with fibrosis subtypes are only partly understood.

We investigated myocardial fibrosis in a large series of symptomatic severe AS patients using invasive biopsy and non-invasive imaging. We simultaneously and at scale assessed cardiac status by measuring functional capacity and blood biomarkers (cardiomyocyte stress/damage markers), by imaging structure and function (echocardiography and CMR), and by performing non-invasive (ECV and LGE) and histological (fibrosis location, pattern, and CVF) tissue characterization.

Methods

Study cohort

A single centre, prospective observational cohort study at University College London Hospital NHS Trust between January 2012 and January 2015 of patients with severe, symptomatic AS undergoing surgical aortic valve replacement (AVR) with or without coronary artery bypass grafting (CABG) using invasive and non-invasive assessment. The study was approved by the ethical committee of UK National Research Ethics Service (07/H0715/101) and was performed as a planned sub-study of RELIEF-AS (ClinicalTrials.gov NCT02174471). The study conformed to the principles of the Helsinki Declaration, and all subjects gave written consent to participate. Patients were recruited prior to pre-operative assessment and underwent clinical assessment with clinical history, blood pressure, 6-minute-walk test (6MWT), blood sampling [for haematocrit, renal function, N-terminal pro-brain natriuretic peptide (NT-proBNP) and high sensitivity troponin T (hs-TnT)], transthoracic echocardiogram, and CMR.

Inclusion criteria: patients undergoing AVR ± CABG for severe AS (two or more of: AVA <1 cm^2, pressure gradient ≥64 mmHg (peak)/ ≥40 mmHg (mean), velocity time integral (VTI) ratio <0.25 or reclassification of discordant echocardiographic data to severe by alternate modality); consenting for study protocol; age >18 years, ability to undergo CMR scan.

Exclusion criteria: pregnancy/breastfeeding, estimated glomerular filtration rate <30 mL/min, CMR incompatible devices, previous valve surgery, infective endocarditis, severe valve disease other than AS or other planned concurrent valve operations (severe AS with mild or moderate AR was acceptable).

Control myocardial samples were obtained from autopsies of 10 subjects (7 male, 3 female; all Caucasian, age: 60 ± 7 years) who died of non-cardiovascular causes showing no signs of macroscopic or microscopic cardiac lesions.

Cardiac imaging

Echocardiography assessed diastolic function and valve area/velocities (with CMR for regurgitant volumes if needed).[13] Cardiovascular magnetic resonance assessed structure, function and myocardial tissue characterization. Echocardiography used a GE Vivid E9 system (GE Healthcare, Wauwatosa, USA) with a 4-MHz transducer as per current guidelines. Cardiovascular magnetic resonance was performed at 1.5 Tesla (Magnetom Avanto, Siemens Medical Solutions) with 32 channel cardiac coil arrays, using a standard clinical scan protocol with LGE imaging and T1 mapping prior to and after bolus gadolinium contrast [0.1 mmol/kg of Gadoterate meglumine (gadolinium-DOTA, marketed as Dotarem, Guerbet S.A., Paris, France)]. Post-contrast imaging was performed at 10 min (LGE) and 15 min (T1 mapping). The T1 mapping sequence used was a balanced-SSFP-based *MO*dified *Look-Locker Inversion Recovery* (MOLLI) variants (investigational prototypes) with motion-correction (sampling scheme pre-contrast 5s(3s)3s and post-contrast 4s(1s)3s(1s)2s; system software version VB17).[14]

Image analysis

Cardiovascular magnetic resonance imaging analysis was performed using CVI42 software (Version 5.1.2[303], Calgary, Canada) blinded to clinical parameters. Left ventricular volume and mass analysis were performed by manual contouring of the endo- and epicardial borders at end-diastole and end-systole with papillary muscle and trabeculations included in the LV mass. Late gadolinium enhancement was quantified in grams and percentage of LV mass using a 3 standard deviations (SD) threshold. For T1 mapping, three short axis T1 maps (base, mid, and apex) were manual contoured for endo- and epicardial borders. Partial voluming of blood was minimized by an automatic 10% offset from the endo- and epicardial border (see Supplementary material online, *Figure S2*). Segments with infarct-pattern LGE (subendocardial LGE) were excluded from ECV analysis but non-infarct LGE was included (as per guidelines). Extracellular volume fraction was defined as $ECV = (1\text{-Hct}) \times [\Delta R1_{myocardium}]/[\Delta R1_{blood}]$.[15] Normal ranges have been described previously.[16]

Histomorphological studies

Biopsies were harvested under direct vision from the basal anteroseptum when the native valve was removed by one of six surgeons using either a 14-gauge coaxial needle system (Temno evolution, Carefusion, USA) or a surgical scalpel, as per surgeon's choice (as per ethics) and fixed in 10% buffered formalin and embedded in paraffin. Histological analysis was performed blinded to clinical and imaging data. For MF, the fraction of myocardial volume with positive staining for collagen, CVF, was determined by quantitative morphometry (Cell'D, Olympus Soft imaging Solutions GmbH, Münster, Germany) in sections stained with collagen-specific picrosirius red. All available myocardial tissue was analysed (average area was 5.21 ± 3.62 mm^2/sample).[9] Endocardial thickness was quantified as the mean value of 5–15 measurements.

Table I   Baseline characteristics

	Total
n, male (%)	133 (56%)
Age (years)	70.3 ± 9.6
BMI (kg/m²)	28.3 ± 5.1
Co-morbidities	
Hypertension	101 (76%)
SBP (mmHg)	134 ± 18
DBP (mmHg)	76 ± 11
Diabetes	28 (21%)
Coronary artery disease	45 (34%)
Symptoms (yes/no)	127/6
NYHA functional class I, II, III, IV	26, 62, 41, 4
Chest pain	43 (32%)
Syncope	11 (8%)
Six-minute walk test distance (m; median IQR)	458 (318–572)
Risk scores	
STS % (median IQR)	1.5 (1.0–2.4)
EuroScoreII % (median IQR)	1.6 (1.0–2.5)
Type of valve	
Tricuspid	95 (71%)
Bicuspid	37 (28%)
Unicuspid	1
Echocardiography	
Vmax (m/s)	4.3 ± 0.6
Peak gradient (mmHg)	75 ± 19
Mean gradient (mmHg)	46 ± 13
AVAi (cm²/m²)	0.41 ± 0.13
Diastolic function	
E-wave	0.85 ± 0.29
E deceleration time (ms)	237 ± 75
E/e' ratio	13.7 ± 6.1
PASP (mmHg)	31 ± 8
CMR parameters	
EDVi (mL/m²)	66 ± 22
ESVi (mL/m²)	22 ± 19
LVMi (g/m²)	87 ± 24
LVEF (%)	70 ± 15
SVi (mL/m²)	44 ± 11
CI (L/min/m²)	3.2 ± 0.7
Maximal wall thickness (mm)	14 ± 3
LAAi (cm²/m²)	13.5 ± 3.9
CMR flow	
Aortic regurgitant fraction in %, median IQR	10.9 (3.3–24.3)
Mitral regurgitant fraction in %, median IQR	4.0 (0–20.5)
Late gadolinium enhancement	
3SD method in grams, median IQR	10.5 (6.0–20.3)
T1 mapping (MOLLI)	
T1 myocardium (native in ms)	1043 ± 44
ECV (%)	28.4 ± 2.9
Histology	
Collagen volume fraction (%)	11.5 ± 8.6
Endocardial thickness (μm)	228 ± 129

Continued

Table I   *Continued*

	Total
Drug history	
ACE-I/ARB	60 (45%)
Betablocker	45 (34%)
Statin	86 (65%)
Aspirin	54 (41%)
Spironolactone	3 (2%)
Blood	
NT-pro-BNP (pg/mL) (median IQR)	72 (29–242)
hs-Troponin T (ng/L) (median IQR)	13 (8–19)
Creatinine (micromol/L)	85 ± 26
eGFR (mL/min/1.73m²)	77 ± 22
Haematocrit (%)	40.0 ± 4.2

BSA, body surface area; SBP, systolic blood pressure; DBP, diastolic blood pressure; NYHA, New York Heart Association; IQR, interquartile range; STS, Society of Thoracic Surgeons' risk model score; EuroScoreII, European System for Cardiac Operative Risk Evaluation II score; Vmax, peak velocity through the aortic valve; AVAi, aortic valve area index; E, peak early velocity of the transmitral flow; E', peak early diastolic velocity of the mitral annulus displacement; PASP, pulmonary artery systolic pressure measured by echocardiography; EDVi, end-diastolic volume index; ESVi, end-systolic volume index; LVMi, left ventricular mass index; LVEF, left ventricular ejection fraction; SVi, stroke volume index; CI, cardiac output indexed; LAAi, left atrial area index; 3SD, three standard deviations; ECV, extracellular volume; ACE-I, angiotensin-converting-enzyme inhibitor; ARB, angiotensin-receptor blocker; NT-proBNP, N-terminal pro-brain natriuretic peptide; hs-TnT, high sensitivity troponin T; eGFR, estimated glomerular filtration rate; CMR, cardiovascular magnetic resonance.

Statistical analysis

Statistical analyses used SPSS 22 (IBM, Armonk, NY, USA). Continuous variables were expressed as mean ± SD, categorical as percentages. Normality was checked using the Shapiro–Wilk test. Groups were compared using independent-samples t-test (if normal) or the Mann–Whitney U (if non-normal), and the χ^2 test for binomial variables. Correlations were estimated by using the Pearson correlation coefficient once normality was demonstrated; otherwise, the Spearman correlation coefficient. Log transformation was applied to normalize NT-proBNP and hs-TnT. The influence of potential confounding factors [age, gender, history of coronary artery disease (CAD)] used multivariate linear regression analysis. The unstandardized coefficient B and its 95% confidence interval were recorded. A two-sided P-value of <0.05 was considered significant.

Results

Baseline characteristics

One hundred and forty-four patients with severe, symptomatic AS underwent CMR prior to and myocardial biopsy at the time of AVR. Eleven patients were excluded due to inability to complete CMR [claustrophobia ($n = 2$), haemodynamic instability ($n = 1$)], incomplete CMR dataset ($n = 1$), or significant bystander disease known to affect LV remodelling and outcome (cardiac amyloidosis $n = 6$; Fabry Disease $n = 1$).[17]

One hundred thirty-three patients were included (age 70 ± 10 years, 56% male, AVAi 0.41 ± 0.13 cm²/m², Vmax 4.3 ± 0.6 m/s, mean gradient 46 ± 13 mmHg); all but 6 patients were symptomatic (96%) with dyspnoea (80%), chest pain (32%), and/or syncope (8%). Aetiology of AS was predominantly tricuspid (71%) with the
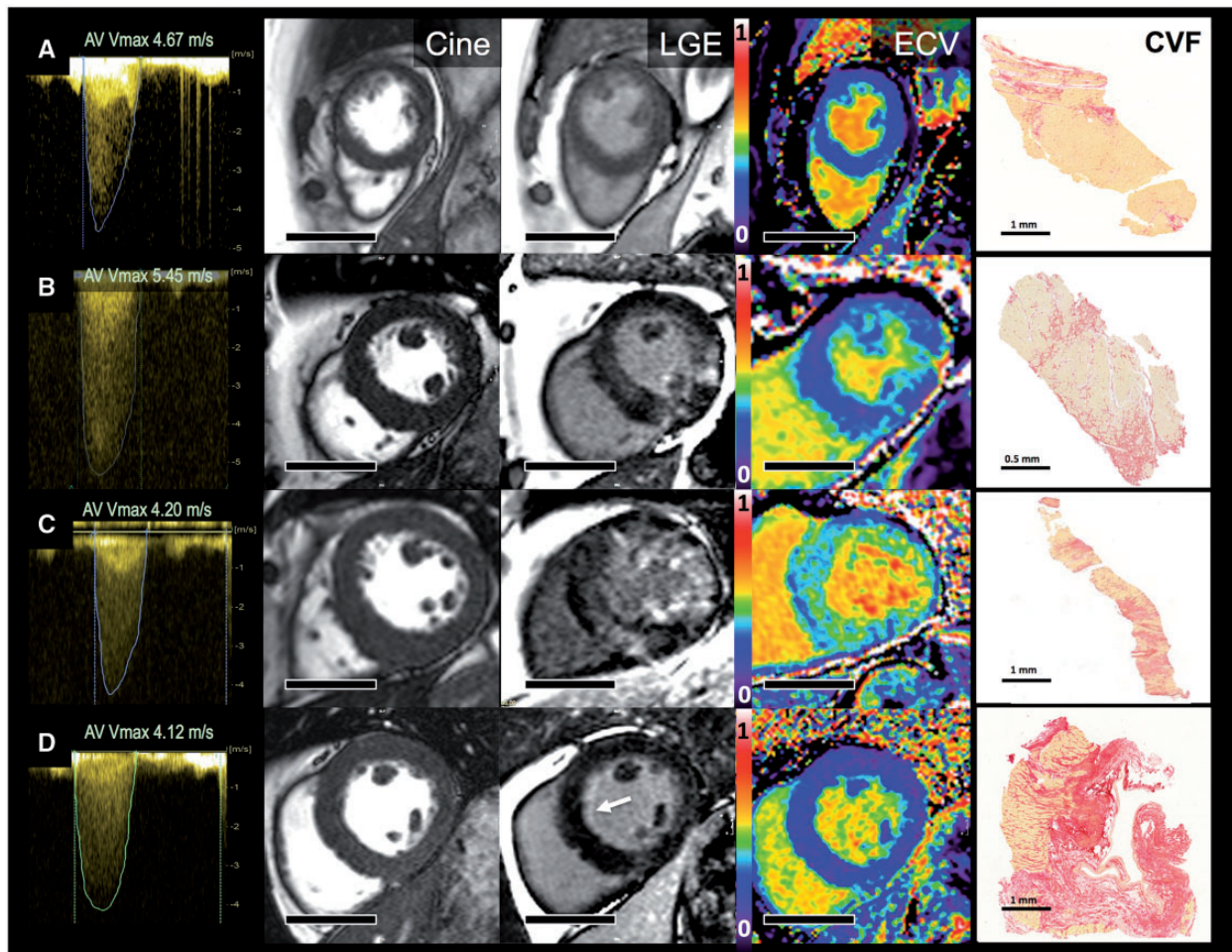
Figure 1 Aortic stenosis, myocardial hypertrophy and fibrosis by imaging and biopsy. Four exemplar patients showing continuous-wave Doppler (maximum velocities >4m/s; Column 1), short axis cine stills demonstrating degrees of left ventricular hypertrophy (Cine; Column 2), matching late gadolinium enhancement images (LGE, Column 3), matching extracellular volume fraction (ECV, Column 4), myocardial biopsy stained with picrosirus red [collagen volume fraction (CVF), Column 5]. Patient A has minimal LVH, no LGE, an ECV of 28.4% and minimal biopsy subendocardial fibrosis (CVF 4.6%). Patient B has concentric LVH, patchy non-infarct LGE, an ECV of 29.9% and moderate biopsy fibrosis (CVF 19.3%). Patient C has concentric LVH, widespread non-infarct LGE, an ECV of 36.5%, and severe biopsy fibrosis (CVF 24.5%). Patient D has mild concentric LVH, subtle subendocardial LGE (white arrow), an ECV of 24.5%, thickened endocardium, and subendocardial scarring. Scale bars (Columns 2–4) equal 5 cm.

remainder bicuspid (28%) or unicuspid AS ($n = 1$). The treatment received was tissue or mechanical valve replacement in 71% and 29%, respectively, with additional bypass grafting in 23% and aortic intervention in 6%. Baseline characteristics are shown in *Table 1*. Representative images of the AS severity by echocardiography (continuous-wave Doppler), LV remodelling (SSFP-cine short axis), and MF by CMR (LGE and ECV) and histology (CVF) are shown in *Figure 1*.

Non-invasive assessment by cardiovascular magnetic resonance

Focal fibrosis, measured by LGE, was commonly seen, affecting 71% of men and 46% of women, with a similar split in infarct-like pattern vs. non-infarct pattern LGE (males 16% vs. 59%; females 17% vs.

37%—some had both). The location of non-infarct LGE was right ventricular insertion point (60%), patchy focal (26%), papillary muscle (19%), and/or mid-myocardial (18%) (see Supplementary material online, *Figure S2*). Mean enhanced LV myocardial mass was $14.3 \pm 11.2\,g$ (median 10.5 g; interquartile range 6.0–20.3 g). Mean ECV was $28.4 \pm 2.9\%$. Imaging findings are summarized in *Table 1*.

Invasive assessment by biopsy

Collagen volume fraction was elevated in severe AS ($11.5 \pm 8.6\%$ vs. $1.95 \pm 0.20\%$ controls, $P < 0.001$) and was higher in men than in women (12.9 ± 8.8 vs. $9.9 \pm 8.0\%$, $P = 0.030$). There were 53 myocardial biopsies with endocardium (mostly from scalpel biopsies, 60%) and 80 samples with no identifiable endocardium. Biopsies with
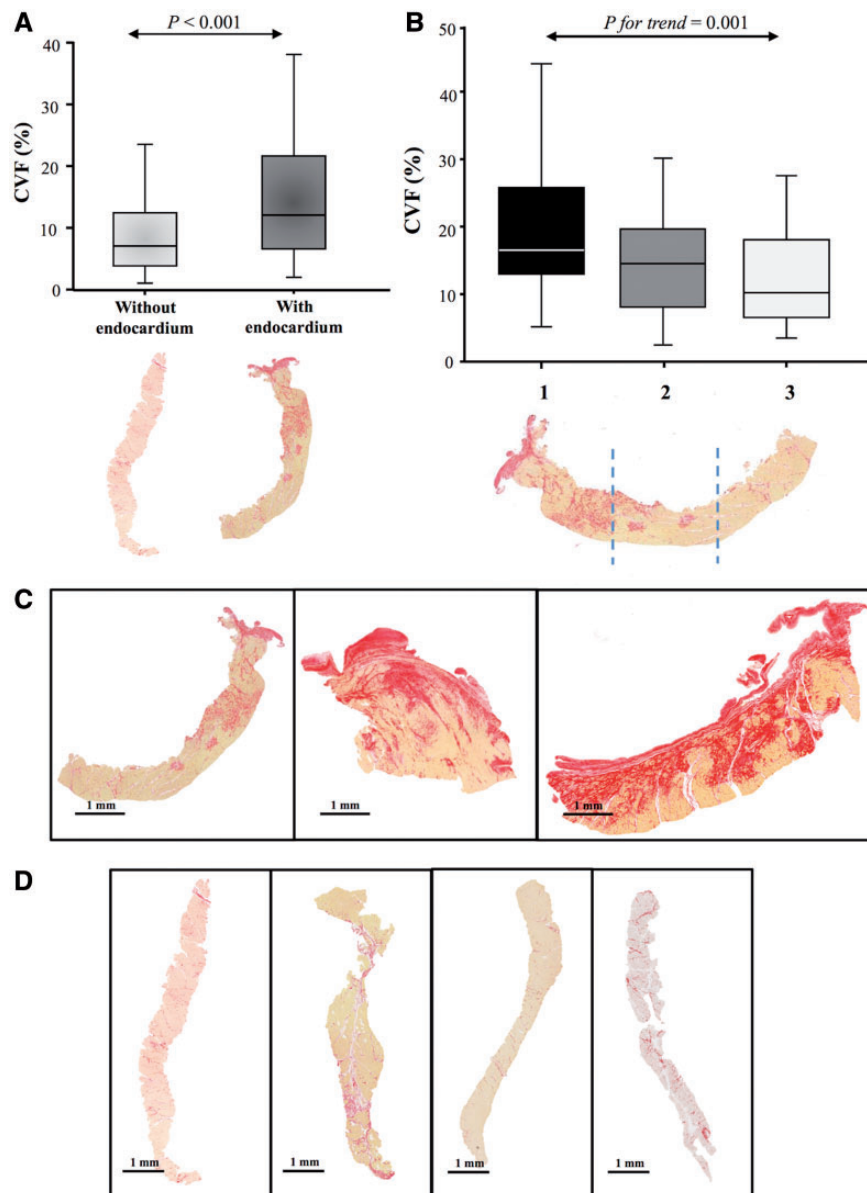
Figure 2 Biopsies with and without endocardium—presence of a gradient of fibrosis. (*A*) Collagen volume fraction in biopsies with and without endocardium. (*B*) Collagen volume fraction in samples with endocardium divided in tertiles. Box plots show the 5th and 95th (vertical lines), 25th and 75th (boxes), and 50th (horizontal line) percentile values for collagen volume fraction. (*C*) Representative images of three biopsies with endocardium (left panel needle and middle and right panel scalpel). (*D*) Representative images of four biopsies without endocardium (needle).

endocardium showed higher CVF than biopsies without endocardium (15.0 ± 12% vs. 8.99 ± 6.7% P < 0.001; *Figure 2*). The endocardium was thickened in AS patients due to collagen deposition in most biopsies, with a mean endocardial thickness of 228 ± 129 microns vs. 40 ± 16 microns in the control samples (P < 0.001; *Figure 3A*). Segmental analysis in tertiles of endocardium-containing biopsies (in those structurally feasible; n = 40) revealed a decreasing gradient of fibrosis from the subendocardium towards the mid-myocardium (20.4 ± 11.3% vs. 15.2 ± 8.7% vs. 13.0 ± 7.8%, *P for trend* = 0.001;

Figure 2). Of note, subendocardial fibrosis was caused predominantly by microscars, whereas mid-myocardial fibrosis was due to interstitial bands preferentially located around cardiomyocytes (*Figure 3B*).

Analysis of associations

Late gadolinium enhancement quantification correlated with CVF in all samples (r^2 = 0.248, P < 0.001), but this association was stronger in endocardial containing samples (r^2 = 0.501, P < 0.001; *Figure 4*). These associations were independent of age, gender and history of CAD.
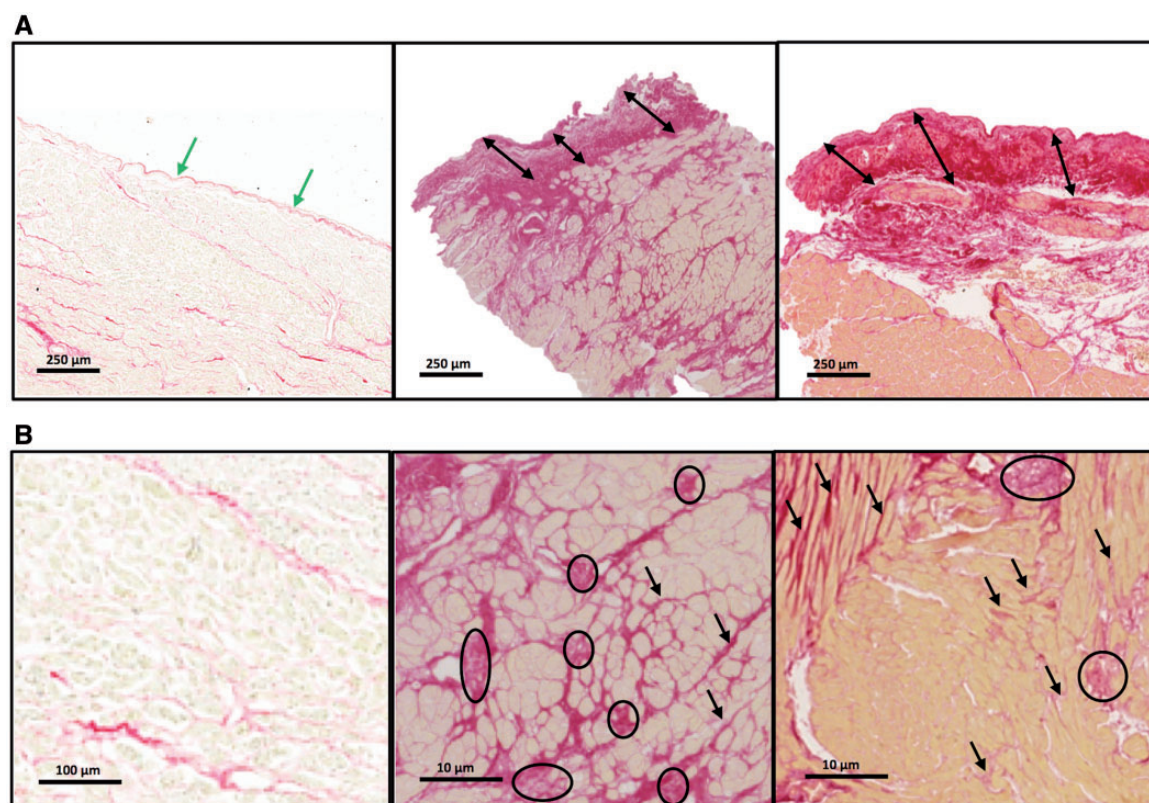
Figure 3 Patterns of fibrosis—endocardial thickening and myocardial microscars and interstitial fibrosis. (*A*) The endocardium in a control subject (left panel) and in two aortic stenosis patients at the same magnification. The arrows show the endocardial thickness (green in normal, black in aortic stenosis). (*B*) Higher magnification showing minimal subendocardial interstitial fibrosis in a control subject (left panel) and extensive microscars and interstitial fibrosis in two aortic stenosis patients. Circles identify microscars and arrows diffuse fibrosis.

Collagen volume fraction quantification was weakly associated with NT-proBNP ($r^2 = 0.055$, $P = 0.013$) and hs-TnT ($r^2 = 0.072$, $P < 0.01$) levels in all patients. The correlation between CVF and NT-proBNP improved slightly when we considered only the endocardial samples ($r^2 = 0.123$, $P = 0.027$). However, these associations were lost when adjusting for confounding factors.

With regards to LV structure and function, both LGE and ECV correlated weakly with LV end-diastolic volume index (LVEDVi; $r^2 = 0.038$, $P = 0.026$ and $r^2 = 0.066$, $P = 0.006$, respectively), LV end-systolic volume index (LVESVi; $r^2 = 0.067$, $P \leq 0.003$ and $r^2 = 0.114$, $P < 0.001$, respectively) and left ventricular ejection fraction (LVEF) ($r^2 = -0.055$, $P = 0.007$ and $r^2 = -0.096$, $P = 0.001$, respectively); but the associations were only independent of confounding factors for ECV. Late gadolinium enhancement was weakly but independently correlated with LVMi ($r^2 = 0.087$, $P = 0.001$); ECV was not ($P = 0.06$).

With regards to biomarkers, both LGE and ECV were independently correlated with NT-proBNP ($r^2 = 0.212$, $P < 0.001$ and $r^2 = 0.307$, $P < 0.001$, respectively; *Figure 5A* and *B*) and hs-TnT ($r^2 = 0.203$, $P < 0.001$ and $r^2 = 0.132$, $P < 0.001$, respectively; *Figure 5C* and *D*).

Aortic stenosis valve severity did not associate with CVF, endocardial thickness, LGE, ECV, NT-proBNP levels, or the degree of LV remodelling. Of LGE, ECV, and CVF, only ECV correlated weakly with the patient functional limitation (6MWT; $r^2 = -0.042$, $P = 0.040$), but this association was lost when adjusting for confounding factors.

To further evaluate the potential confounding effect of CAD, we performed a sensitivity analysis by excluding patients with CAD and we obtained the same results as with the adjusted multivariate linear regression analysis.

Clinical and structural impact of late gadolinium enhancement and extracellular volume fraction stratification

To compare LGE and ECV with clinical and structural parameters, we dichotomized the variables (above and below median: 10.5 g for LGE, 28.4% for ECV) with results shown in *Table 2*.

Patients with high vs. low LGE had more advanced LV remodelling with higher LVESVi ($P = 0.041$), LVEDVi ($P = 0.045$), LV mass index ($P = 0.035$), left atrial area index (LAAi) ($P = 0.006$), lower LVEF ($P = 0.032$), more mitral regurgitation ($P = 0.012$), higher prevalence of hypertension ($P = 0.006$), and CAD ($P = 0.015$). In accordance with
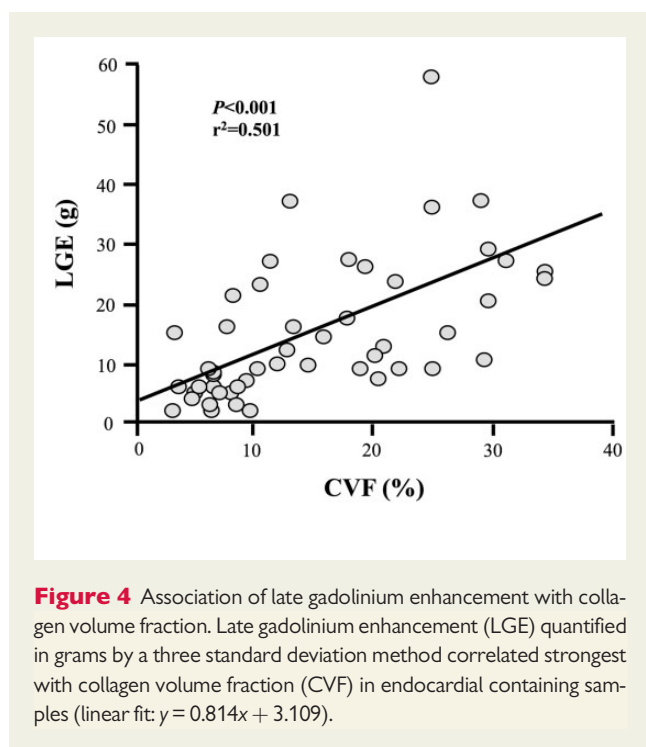
Figure 4 Association of late gadolinium enhancement with collagen volume fraction. Late gadolinium enhancement (LGE) quantified in grams by a three standard deviation method correlated strongest with collagen volume fraction (CVF) in endocardial containing samples (linear fit: $y = 0.814x + 3.109$).

the association analysis, these patients presented higher CVF values ($P < 0.001$), NT-proBNP ($P < 0.001$), and hs-TnT ($P = 0.001$) levels.

Patients with high vs. low ECV also had greater LV remodelling with increased LVEDVi ($P = 0.012$), LVESVi ($P = 0.002$), and lower LVEF ($P = 0.0031$). Although the LAAi was not significantly different ($P = 0.08$), diastolic function was worse (E/A, $P = 0.022$ and E/e' ratio, $P = 0.018$). Moreover, they also had an impaired 6MWT and a higher New York Heart Association functional class. In accordance with the association analysis, these patients presented higher NT-proBNP ($P < 0.001$) and hs-TnT ($P = 0.018$) levels.

Combining LGE and ECV added value (*Table 3*). With increasing abnormality in these parameters, cavity dimensions (LVEDVi, LVESVi, and LAAi) increased, LVEF decreased, NT-proBNP and hs-TnT levels increased, CVF increases, and patient functional capacity (6MWT) decreased ($P = 0.010$). Interestingly, these changes were maintained when we adjusted the analysis by the presence of CAD.

Discussion

In this, the largest prospective AS biopsy and multimodality imaging/biomarker study to date, the main findings are: (i) Histological assessment of the myocardium in severe AS revealed complex morphology and topography of fibrosis with three main patterns: thickened endocardium with a massive fibrotic layer; a fibrosis gradient from the subendomyocardium to the mid-myocardium with abundant microscopic scars; and diffuse interstitial fibrosis. (ii) Neither histological collagen volume fraction nor the CMR parameters ECV and LGE captured this fibrosis in its totality. (iii) The combination of LGE and ECV identified better those AS patients presenting with more adverse LV remodelling, more altered blood biomarkers and histological parameters, and a more

reduced functional capacity than each parameter alone (*Summarizing Illustration*). These findings were independent of the presence of CAD.

Biopsy findings

In the last 40 years, several studies have described MF as histological hallmark of severe AS, documenting relevant clinical correlations and an important prognostic role.[3,18–21] However, these studies were small and patient demographics have dramatically changed since the early landmark studies in the 1970s and 80s ($n \sim 20$, mean age ~ 50, predominantly male).[18–21] Furthermore, the methodology of fibrosis assessment has advanced since then. Our study used current histological techniques to systematically evaluate MF in severe AS not only quantitatively but also morphologically and topographically in a large cohort of patients reflecting the changing patients demographics in AS ($n = 133$, mean age 70, 56% male).

We confirm the existence of a decreasing collagen gradient from endocardium to the mid-myocardium in severe AS, supporting prior studies.[18,19] Importantly, the scalpel biopsies showed this better than needle biopsies as they have higher yield of endocardium (needed to orientate the sample).

The different patterns of collagen in severe AS may have different pathogenic mechanisms and possible consequences. Most collagen deposits exist as a thickened endocardial layer and subendocardial scattered microfoci and trabecular fibrosis. Mid-myocardial fibrosis appears as a diffuse network around cardiomyocytes and bundles. The fibrosis gradient may be related to low-endocardial perfusion,[19] thus reflecting a reparative response (i.e. replacement fibrosis) to ischaemia and subsequent cell loss. This is supported by previous findings showing that reduced capillary density, in absolute terms as well as in relation to the number of cardiomyocytes, accompanies MF in patients with severe AS.[22] On the other hand, the diffuse MF located around cardiomyocytes may be reactive to pressure overload-induced mechanical stimulation of local fibroblasts and to paracrine factors produced by mechanically stressed (strain) cardiomyocytes that, in turn, stimulate fibroblasts (i.e. reactive fibrosis).[23]

Cardiovascular magnetic resonance findings

Cardiovascular magnetic resonance tissue characterization has developed over two decades, initially with the LGE technique for focal fibrosis,[4–8] later with the ECV technique for diffuse fibrosis.[9–12,24] Combined biopsy and CMR study are rare and limited by small sample size. Instead, myocardial tissue characterization in AS has been described by presence or absence, and pattern of LGE (subendocardial infarct-pattern vs. mid-wall non-infarct LGE). These histological findings of thickened endocardium and a gradient of myocardial fibrosis from endo- to epicardium suggest that these descriptive LGE pattern need to be revisited, possibly by utilizing the latest motion-correction or dark blood techniques.[25]

Here, LGE correlated with CVF (although the biopsy was obtained from the basal anteroseptum which was not infarcted in any patient), especially on endocardial biopsies ($r^2 = 0.5$), which capture more of the subendocardial microscars. The ECV was only mildly elevated with broadly proportional increase in the cellular and extracellular components of the myocardium (as observed by Schwarz *et al.*[18] in 1978), and, unlike other papers, did not correlate with CVF.
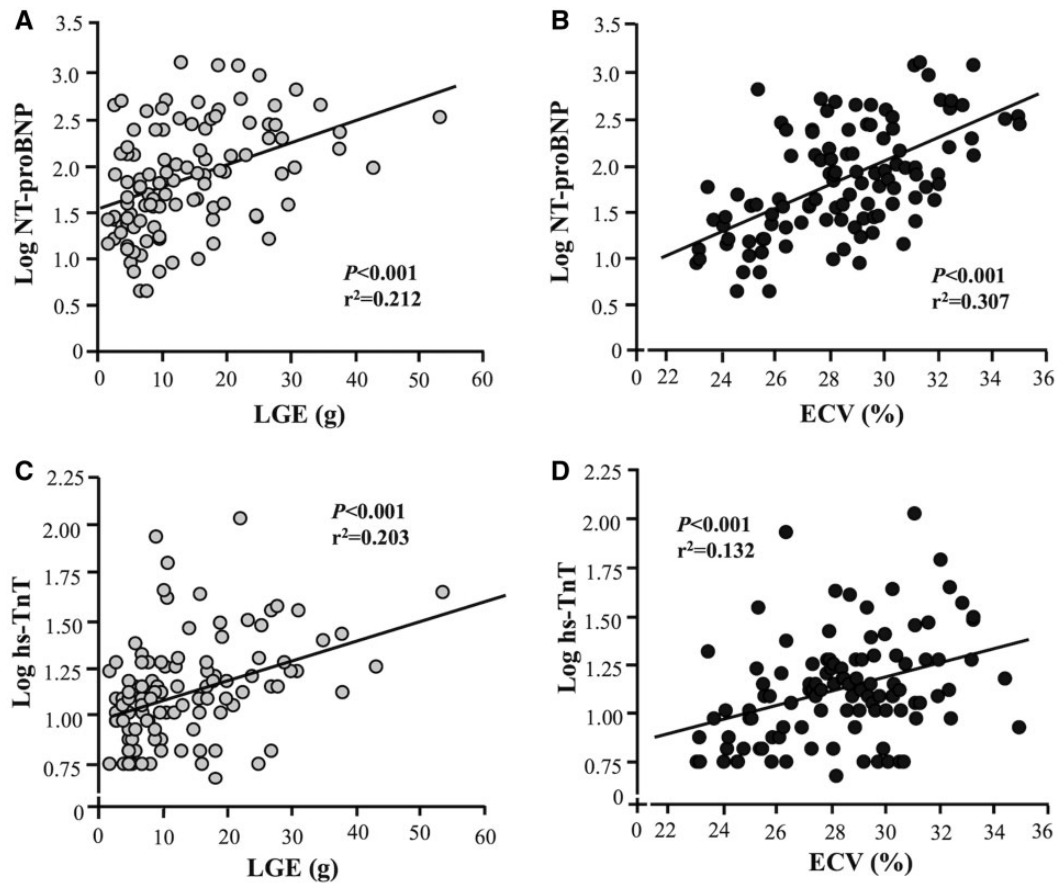
Figure 5 Associations of imaging and blood biomarkers. Late gadolinium enhancement (LGE) and extracellular volume fraction (ECV) correlated with NT-proBNP (*A* and *B*) and with hs-TnT (*C* and *D*) (linear fit: A $y = 0.119x - 1.498$; B $y = 0.037x + 0.103$; C $y = 0.025x + 1.567$; D $y = 0.110x + 1.008$).
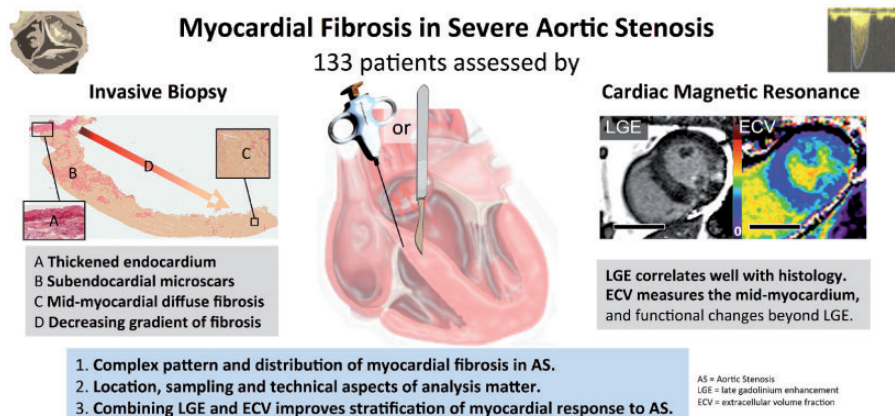
Summarizing Illustration This figure summarizes the main findings of the study.

Table 2 Patients stratified according to late gadolinium enhancement or extracellular volume median value

	LGE			ECV		
	<10.5 g (n = 65)	> =10.5 g (n = 66)	P-value	<28.4% (n = 58)	> =28.4% (n = 58)	P-value
Age (years)	68.8 ± 10.4	71.7 ± 8.8	0.089	70.3 ± 10.0	70.1 ± 9.7	0.910
Gender (male/female)	28/37	45/21	**0.004**	34/24	31/27	0.575
BMI (kg/m^2)	28.7 ± 5.5	28.2 ± 4.7	0.567	27.8 ± 5.0	29.3 ± 5.0	0.097
Comorbidities, n (%)						
HTN	44 (68%)	56 (89%)	**0.006**	43 (75%)	49 (84%)	0.225
AF	6 (9%)	13 (20%)	0.089	7 (12%)	11 (19%)	0.305
CAD	14 (22%)	29 (45%)	**0.015**	19 (33%)	21 (36%)	0.746
Symptom, n (%)						
Syncope	6 (9%)	4 (6%)	0.600	6 (10%)	4 (7%)	0.489
NYHA			0.721			**0.040**
I	8 (12%)	9 (14%)		8 (14%)	5 (9%)	
II	33 (51%)	28 (42%)		34 (59%)	24 (41%)	
III	17 (26%)	23 (35%)		13 (22%)	21 (36%)	
IV	2 (3%)	2 (3%)		0 (0%)	4 (7%)	
Chest pain			0.288			0.982
0	41 (63%)	39 (59%)		35 (60%)	37 (64%)	
1	3 (5%)	7 (11%)		5 (9%)	5 (9%)	
2	15 (23%)	8 (12%)		12 (21%)	10 (18%)	
3	4 (6%)	5 (8%)		4 (7%)	5 (9%)	
Valve type, bi/tri (n)	20/45	18/48	0.659	16/42	17/41	0.837
AVAi (cm^2/m^2)	0.41 ± 0.14	0.40 ± 0.13	0.605	0.42 ± 0.15	0.39 ± 0.11	0.384
Mean gradient (mmHg)	44.8 ± 11.9	47.8 ± 14.7	0.216	47.1 ± 14	44.8 ± 13	0.368
Mitral regurgitation (%)	7.4 ± 11.2	15.2 ± 14.3	**0.012**	9.1 ± 12.7	11.5 ± 12.9	0.428
EDVi (mL/m^2)	63.2 ± 20.9	70.2 ± 21.9	**0.045**	61.0 ± 19.1	71.4 ± 24.7	**0.012**
ESVi (mL/m^2)	19.0 ± 15.6	25.6 ± 20.7	**0.041**	16.9 ± 12.0	27.7 ± 23.3	**0.002**
LVMi (g/m^2)	83.9 ± 27.5	90.7 ± 20.7	**0.035**	83.7 ± 24.4	91.8 ± 25.6	0.085
LVEF (%)	72.4 ± 13.2	67.1 ± 15.4	**0.032**	73.9 ± 11.4	65.6 ± 17.0	**0.003**
MAPSE (mm)	10.7 ± 3.5	9.8 ± 3.6	0.123	11.0 ± 3.2	9.53 ± 3.7	**0.031**
LAAi (cm^2/m^2)	12.7 ± 3.3	14.5 ± 4.2	**0.006**	12.8 ± 3.3	14.4 ± 4.6	0.081
E/A	0.91 ± 0.42	1.08 ± 0.58	0.084	0.87 ± 0.38	1.10 ± 0.59	**0.022**
DT (ms)	245 ± 69	227 ± 82	0.206	236 ± 72	237 ± 81	0.940
E/e'	13.57 ± 6.28	13.94 ± 6.11	0.771	12.46 ± 6.27	14.94 ± 5.96	**0.018**
6MWT (m)	468 ± 190	412 ± 187	0.143	488 ± 145	393 ± 210	**0.006**
ECV (%)	27.5 ± 2.6	29.5 ± 2.8	**<0.001**	26.0 ± 1.7	30.7 ± 1.8	**<0.001**
LGE (g)	5.84 ± 2.5	22.8 ± 9.9	**<0.001**	11.5 ± 9.1	15.4 ± 12.2	0.090
CVF (%)	7.3 ± 4.7	15.7 ± 9.8	**<0.001**	10.4 ± 7.5	10.9 ± 8.5	0.707
NT-proBNP (pg/mL)	96 ± 139	277 ± 341	**<0.001**	99 ± 154	262 ± 335	**<0.001**
hs-TnT (ng/L)	15 ± 10	21 ± 20	**0.001**	15 ± 13	21 ± 18	**0.018**

Boldface values indicate statistically significant P-values.
Values are given as mean ± SD or n (and percentage).
LGE, late gadolinium enhancement; ECV, extracellular volume; BMI, body mass index; HTN, hypertension; AF, atrial fibrillation; CAD, coronary arterial disease; EDVi, end-diastolic volume index; ESVi, end-systolic volume index; LVMi, left ventricular mass index; LVEF, left ventricular ejection fraction; MAPSE, mitral annular plane systolic excursion; LAAi, left atrial area index; E, peak early velocity of the transmitral flow; A, peak late velocity of the transmitral flow; DT, deceleration time; E', peak early diastolic velocity of the mitral annulus displacement; 6MWT, 6-minute-walk test; bi, bicuspid; tri, tricuspid; AVAi, aortic valve area index; CVF, collagen volume fraction; NT-proBNP, N-terminal pro-brain natriuretic peptide; hs-TnT, high sensitivity troponin T; SD, standard deviation; NYHA, New York Heart Association.

However, ECV did capture functionally important consequences, given that patients with high ECV showed worse NT-ProBNP, 6MWT, and NYHA functional class.[9–12,24] There are a number of possible reasons for this discordance with other studies including the underestimation of subendocardial microscar and fibrosis gradient due to avoidance of the endo- and epicardium (for ECV we eroded 10% from the edge to avoid blood pool contamination); recruitment of a less severe (more representative) phenotypes with less extensive scarring (we recruited 50% of all AVR in our institution); reduced capillary density (lower ECV) or compensatory vasodilatation (higher ECV) may confound ECV measurements, which captures all extracellular space including the intravascular plasma.[26,27]

We suspect that LGE is a marker of the reparative fibrotic response to cardiomyocyte injury and loss. On the other hand, diffuse

Table 3   Patients stratified according to extracellular volume and late gadolinium enhancement combined

	ECV−/LGE− (n = 37)	ECV−/LGE+ & ECV+/LGE− (n = 46)	ECV+/LGE+ (n = 32)	*P*-value
Age (years)	68.6 ± 11.0	71.4 ± 9.0	70.4 ± 9.8	0.421
Gender (male/female)	19/18	24/22	22/10	0.259
BMI (kg/m^2)	28.3 ± 5.3	28.4 ± ± 5.4	29.0 ± 4.5	0.594
Comorbidities, *n* (%)				
HTN	24 (65%)	38 (83%)	29 (91%)	**0.041**
AF	3 (8%)	7 (15%)	8 (25%)	0.243
CAD	7 (19%)	18 (39%)	14 (44%)	0.072
Symptom, *n* (%)				
Syncope	5 (14%)	2 (4%)	3 (9.7%)	0.295
NYHA				0.125
I	5 (14%)	6 (13%)	2 (6%)	
II	24 (65%)	17 (37%)	16 (50%)	
III	16 (43%)	18 (39%)	10 (31%)	
IV	0 (0%)	2 (4%)	2 (6%)	
Chest pain				0.583
0	23 (62%)	27 (59%)	21 (66%)	
1	2 (5%)	4 (9%)	4 (13%)	
2	9 (24%)	9 (20%)	5 (16%)	
3	1 (3%)	6 (13%)	2 (6%)	
Valve type, bi/tri (n)	12/25	12/34	9/23	0.814
AVAi (cm^2/m^2)	0.42 ± 0.16	0.40 ± 0.12	0.39 ± 0.13	0.329
Mean gradient (mmHg)	45.2 ± 14.1	46.7 ± 11.2	45.8 ± 16.6	0.851
Mitral regurgitation (%)	6.8 ± 12.3	10.3 ± 11.4	15.1 ± 15.2	**0.042**
EDVi (mL/m^2)	59.5 ± 20.8	66.8 ± 18.7	73.9 ± 27.2	**0.008**
ESVi (mL/m^2)	15.5 ± 11.3	22.5 ± ± 17.1	30.5 ± 25.9	**0.001**
LVMi (g/m^2)	81.8 ± 26.5	87.3 ± 26.1	95.7 ± 20.9	**0.023**
LVEF (%)	75.4 ± 9.4	69.0 ± 15.0	63.6 ± ± 17.4	**0.001**
MAPSE (mm)	11.3 ± 3.2	10.1 ± 3.5	9.2 ± 3.8	**0.014**
LAAi (cm^2/m^2)	12.4 ± 3.3	13.3 ± 3.1	15.6 ± 5.2	**0.001**
E/A	0.84 ± 0.26	0.97 ± 0.54	1.24 ± 0.63	**0.004**
DT (ms)	240 ± 68	243 ± 76	220 ± 88	0.364
E/e'	13.09 ± 6.83	13.04 ± 5.47	15.60 ± 6.51	0.192
6MWT (m)	512 ± 136	420 ± 207	391 ± 188	**0.010**
ECV (%)	25.6 ± 1.6	28.7 ± 2.1	31.2 ± 1.9	**<0.001**
LGE (grams)	6.01 ± 2.48	12.64 ± 9.67	23.16 ± 11.22	**<0.001**
CVF (%)	7.84 ± 5.01	10.26 ± 8.03	14.45 ± 9.45	**0.001**
NT-proBNP (pg/mL)	60 ± 90	160 ± 189	342 ± 394	**<0.001**
hs-TnT (ng/L)	13.5 ± 14.5	17.5 ± 12.2	23.6 ± 20.4	**0.012**

Boldface values indicate statistically significant *P*-values.
Values are given as mean ± SD or *n* (and percentage).
LGE, late gadolinium enhancement; ECV, extracellular volume; BMI, body mass index; HTN, hypertension; AF, atrial fibrillation; CAD, coronary arterial disease; EDVi, end-diastolic volume index; ESVi, end-systolic volume index; LVMi, left ventricular mass index; LVEF, left ventricular ejection fraction; MAPSE, mitral annular plane systolic excursion; LAAi, left atrial area index; *E*, peak early velocity of the transmitral flow; *A*, peak late velocity of the transmitral flow; DT, deceleration time; *E'*, peak early diastolic velocity of the mitral annulus displacement; 6MWT, 6-minute-walk test; bi, bicuspid; tri, tricuspid; AVAi, aortic valve area index; CVF, collagen volume fraction; NT-proBNP, N-terminal of pro-brain natriuretic peptide; hs-TnT, high sensitivity troponin T; NYHA, New York Heart Association.

reactive interstitial fibrosis is intimately linked to its local environment and depends on cardiomyocyte function, strain and its interactions with fibroblasts. Extracellular volume fraction may therefore be more closely linked to the cardiomyocyte stress, and accordingly could be considered more a measure of cardiomyocyte-interstitial relationship than the current mainstream concept of ECV being a pure interstitial marker.

Clinical impact

Myocardial fibrosis in severe AS has a characteristic pattern and distribution. When measuring MF by biopsy or CMR, location, sampling and technical aspects of analysis matter. Invasive biopsy is limited by size and sampling error, whereas LGE and ECV capture different regions of myocardium and provide complementary information. Both

ECV and LGE track cardiomyocyte stress (NT-proBNP) and injury (hs-TnT). Late gadolinium enhancement is known to track troponin concentrations in AS which has been associated with advanced hypertrophy, replacement fibrosis and outcome.[28] Data on BNP vs. ECV in AS are lacking. Blood biomarkers reflect 'whole heart' cardiomyocyte stress and injury, but need to be interpreted in conjunction with structural and functional parameters from non-invasive imaging, as they can be elevated due to other causes. The imaging biomarkers LGE and ECV offer global but also regional insights—asymmetrical remodelling is common in AS and is associated with increased myocardial injury, left ventricular decompensation, and adverse events.[29] The combination of LGE and ECV—a multi-parametric approach— better identified worse adverse LV remodelling, altered biochemical and histological parameters, and functional capacity than each parameter alone. Timing of AVR is one of the challenges in AS, in particular in asymptomatic patients. Recent focus has turned towards the complex interplay between the degree of the valve stenosis, haemodynamic load, and myocardial response. The combination of LGE and ECV may prove to help in a better understanding of this interplay.

Strengths and limitations

This is the largest combined histology-multimodality imaging study in AS, with even sub-groups larger than previous (n ~20) histological and combined studies.[9–11,18–21] The analysis of the imaging and histological data was performed completely blinded by independent groups. To make this study as applicable as possible, we recruited all-comers (50% of all AVR for AS in our institution) rather than the severe end of the spectrum and thereby included patient with CAD, hypertension and diabetes. The effect of CAD was adjusted for as detailed in the methods. Furthermore, the location of the biopsy (basal anteroseptum) was never infarcted in this study. To achieve a standardized biopsy procedure, all biopsies were obtained under direct vision from the basal anteroseptum by a team of experienced surgeons using either a scalpel or needle technique. Finally, we are aware that alterations in other components of the myocardium (i.e. cardiomyocytes and microvessels) also play a role in the myocardial response to pressure overload and their impacts deserves to be evaluated in further studies.

Conclusion

Myocardial fibrosis in severe AS is complex with three main alterations: endocardial thickening, subendocardial microscars, and diffuse interstitial fibrosis. Neither histological collagen volume fraction nor the CMR parameters ECV and LGE capture this fibrosis in its totality. This study supports that the combination of invasive and non-invasive techniques at scale is relevant to better characterize MF in severe AS patients. Importantly, the combination LGE and ECV allows a better phenotyping of AS patients according to their myocardial response to AS in terms of MF and morphological and functional cardiac alterations.

Supplementary material

Supplementary material is available at *European Heart Journal* online.

Acknowledgements

Funding

References

1. Dweck MR, Boon NA, Newby DE. Calcific aortic stenosis: a disease of the valve and the myocardium. *J Am Coll Cardiol* 2012;**60**:1854–1863.

2. Authors/Task Force Members, Vahanian A, Alfieri O, Andreotti F, Antunes MJ, Baron-Esquivias G, Baumgartner H. Guidelines on the management of valvular heart disease (version 2012): the Joint Task Force on the Management of Valvular Heart Disease of the European Society of Cardiology (ESC) and the European Association for Cardio-Thoracic Surgery (EACTS). *Eur Heart J* 2012;**33**:2451–2496.

3. Villari B, Campbell SE, Hess OM, Mall G, Vassalli G, Weber KT, Krayenbuehl HP. Influence of collagen network on left ventricular systolic and diastolic function in aortic valve disease. *J Am Coll Cardiol* 1993;**22**:1477–1484.

4. Azevedo CF, Nigri M, Higuchi ML, Pomerantzeff PM, Spina GS, Sampaio RO, Tarasoutchi F, Grinberg M, Rochitte CE. Prognostic significance of myocardial fibrosis quantification by histopathology and magnetic resonance imaging in patients with severe aortic valve disease. *J Am Coll Cardiol* 2010;**56**:278–287.

5. Dweck MR, Joshi S, Murigu T, Alpendurada F, Jabbour A, Melina G, Banya W, Gulati A, Roussin I, Raza S, Prasad NA, Wage R, Quarto C, Angeloni E, Refice S, Sheppard M, Cook SA, Kilner PJ, Pennell DJ, Newby DE, Mohiaddin RH, Pepper J, Prasad SK. Midwall fibrosis is an independent predictor of mortality in patients with aortic stenosis. *J Am Coll Cardiol* 2011;**58**:1271–1279.

6. Barone-Rochette G, Pierard S, De Meester de Ravenstein C, Seldrum S, Melchior J, Maes F, Pouleur AC, Vancraeynest D, Pasquet A, Vanoverschelde JL, Gerber BL. Prognostic significance of LGE by CMR in aortic stenosis patients undergoing valve replacement. *J Am Coll Cardiol* 2014;**64**:144–154.

7. Weidemann F, Herrmann S, Stork S, Niemann M, Frantz S, Lange V, Beer M, Gattenlohner S, Voelker W, Ertl G, Strotmann JM. Impact of myocardial fibrosis in patients with symptomatic severe aortic stenosis. *Circulation* 2009;**120**:577–584.

8. Herrmann S, Stork S, Niemann M, Lange V, Strotmann JM, Frantz S, Beer M, Gattenlohner S, Voelker W, Ertl G, Weidemann F. Low-gradient aortic valve stenosis myocardial fibrosis and its influence on function and outcome. *J Am Coll Cardiol* 2011;**58**:402–412.

9. Flett AS, Hayward MP, Ashworth MT, Hansen MS, Taylor AM, Elliott PM, McGregor C, Moon JC. Equilibrium contrast cardiovascular magnetic resonance for the measurement of diffuse myocardial fibrosis: preliminary validation in humans. *Circulation* 2010;**122**:138–144.

10. de Meester de Ravenstein C, Bouzin C, Lazam S, Boulif J, Amzulescu M, Melchior J, Pasquet A, Vancraeynest D, Pouleur AC, Vanoverschelde JL, Gerber BL. Histological Validation of measurement of diffuse interstitial myocardial fibrosis by myocardial extravascular volume fraction from Modified Look-Locker imaging (MOLLI) T1 mapping at 3 T. *J Cardiovasc Magn Reson* 2015;**17**:48.

11. White SK, Sado DM, Fontana M, Banypersad SM, Maestrini V, Flett AS, Piechnik SK, Robson MD, Hausenloy DJ, Sheikh AM, Hawkins PN, Moon JC. T1 mapping

for myocardial extracellular volume measurement by CMR: bolus only versus primed infusion technique. *JACC Cardiovasc Imaging* 2013;**6**:955–962.

12. Lee SP, Lee W, Lee JM, Park EA, Kim HK, Kim YJ, Sohn DW. Assessment of diffuse myocardial fibrosis by using MR imaging in asymptomatic patients with aortic stenosis. *Radiology* 2015;**274**:359–369.

13. Baumgartner HC, Hung JC-C, Bermejo J, Chambers JB, Edvardsen T, Goldstein S, Lancellotti P, LeFevre M, Miller F Jr, Otto CM. Recommendations on the echocardiographic assessment of aortic valve stenosis: a focused update from the European Association of Cardiovascular Imaging and the American Society of Echocardiography. *Eur Heart J Cardiovasc Imaging* 2017;**18**:254–275.

14. Kellman P, Arai AE, Xue H. T1 and extracellular volume mapping in the heart: estimation of error maps and the influence of noise on precision. *J Cardiovasc Magn Reson* 2013;**15**:56.

15. Moon JC, Messroghli DR, Kellman P, Piechnik SK, Robson MD, Ugander M, Gatehouse PD, Arai AE, Friedrich MG, Neubauer S, Schulz-Menger J, Schelbert EB; Society for Cardiovascular Magnetic Resonance I, Cardiovascular Magnetic Resonance Working Group of the European Society of C. Myocardial T1 mapping and extracellular volume quantification: a Society for Cardiovascular Magnetic Resonance (SCMR) and CMR Working Group of the European Society of Cardiology consensus statement. *J Cardiovasc Magn Reson* 2013;**15**:92.

16. Kawel-Boehm N, Maceira A, Valsangiacomo-Buechel ER, Vogel-Claussen J, Turkbey EB, Williams R, Plein S, Tee M, Eng J, Bluemke DA. Normal values for cardiovascular magnetic resonance in adults and children. *J Cardiovasc Magn Reson* 2015;**17**:29.

17. Treibel TA, Fontana M, Gilbertson JA, Castelletti S, White SK, Scully PR, Roberts N, Hutt DF, Rowczenio DM, Whelan CJ, Ashworth MA, Gillmore JD, Hawkins PN, Moon JC. Occult transthyretin cardiac amyloid in severe calcific aortic stenosis: prevalence and prognosis in patients undergoing surgical aortic valve replacement. *Circ Cardiovasc Imaging* 2016;**9**:54–63.

18. Schwarz F, Flameng W, Schaper J, Langebartels F, Sesto M, Hehrlein F, Schlepper M. Myocardial structure and function in patients with aortic valve disease and their relation to postoperative results. *Am J Cardiol* 1978;**41**:661–669.

19. Cheitlin MD, Robinowitz M, McAllister H, Hoffman JI, Bharati S, Lev M. The distribution of fibrosis in the left ventricle in congenital aortic stenosis and coarctation of the aorta. *Circulation* 1980;**62**:823–830.

20. Hess OM, Ritter M, Schneider J, Grimm J, Turina M, Krayenbuehl HP. Diastolic stiffness and myocardial structure in aortic valve disease before and after valve replacement. *Circulation* 1984;**69**:855–865.

21. Krayenbuehl HP, Hess OM, Monrad ES, Schneider J, Mall G, Turina M. Left ventricular myocardial structure in aortic valve disease before, intermediate, and late after aortic valve replacement. *Circulation* 1989;**79**:744–755.

22. Moreno MU, Gallego I, Lopez B, Gonzalez A, Fortuno A, San Jose G, Valencia F, Gomez-Doblas JJ, de Teresa E, Shah AM, Diez J, Zalba G. Decreased Nox4 levels in the myocardium of patients with aortic valve stenosis. *Clin Sci (Lond)* 2013;**125**:291–300.

23. Pellman J, Zhang J, Sheikh F. Myocyte-fibroblast communication in cardiac fibrosis and arrhythmias: mechanisms and model systems. *J Mol Cell Cardiol* 2016;**94**:22–31.

24. Bull S, White SK, Piechnik SK, Flett AS, Ferreira VM, Loudon M, Francis JM, Karamitsos TD, Prendergast BD, Robson MD, Neubauer S, Moon JC, Myerson SG. Human non-contrast T1 values and correlation with histology in diffuse fibrosis. *Heart* 2013;**99**:932–937.

25. Kellman P, Xue H, Olivieri LJ, Cross RR, Grant EK, Fontana M, Ugander M, Moon JC, Hansen MS. Dark blood late enhancement imaging. *J Cardiovasc Magn Reson* 2016;**18**:77.

26. Rakusan K, Flanagan MF, Geva T, Southern J, Van Praagh R. Morphometry of human coronary capillaries during normal growth and the effect of age in left ventricular pressure-overload hypertrophy. *Circulation* 1992;**86**:38–46.

27. Mahmod M, Piechnik SK, Levelt E, Ferreira VM, Francis JM, Lewis A, Pal N, Dass S, Ashrafian H, Neubauer S, Karamitsos TD. Adenosine stress native T1 mapping in severe aortic stenosis: evidence for a role of the intravascular compartment on myocardial T1 values. *J Cardiovasc Magn Reson* 2014;**16**:92.

28. Chin CW, Shah AS, McAllister DA, Joanna Cowell S, Alam S, Langrish JP, Strachan FE, Hunter AL, Maria Choy A, Lang CC, Walker S, Boon NA, Newby DE, Mills NL, Dweck MR. High-sensitivity troponin I concentrations are a marker of an advanced hypertrophic response and adverse outcomes in patients with aortic stenosis. *Eur Heart J* 2014;**35**:2312–2321.

29. Kwiecinski J, Chin CW, Everett RJ, White AC, Semple S, Yeung E, Jenkins WJ, Shah AS, Koo M, Mirsadraee S, Lang CC, Mills N, Prasad SK, Jansen MA, Japp AG, Newby DE, Dweck MR. Adverse prognosis associated with asymmetric myocardial thickening in aortic stenosis. *Eur Heart J Cardiovasc Imaging* 2017; doi: 10.1093/ehjci/jex052.